Fabrication and power scaling of a 1.7 W Cr:ZnSe waveguide laser

Patrick A. Berry,[1,*] John R. Macdonald,[2] Stephen J. Beecher,[2] Sean A. McDaniel,[3] Kenneth L. Schepler,[1] and Ajoy K. Kar[2]

[1]Air Force Research Laboratory, Wright Patterson Air Force Base, Ohio 45433, USA
[2]Institute of Photonics and Quantum Sciences, Heriot-Watt University, Edinburgh, EH14 4AS, UK
[3]Scientific Applications International Corp., 3745 Pentagon Blvd, Beavercreek, OH 45431, USA
**Patrick.Berry@wpafb.af.mil*

Abstract: We report the fabrication and operation of a Cr:ZnSe buried channel waveguide laser operating at 2500 nm with a linewidth of 10 nm and a maximum power output of 1.7 W. Ultrafast laser inscription is used to fabricate the depressed cladding waveguide in a polycrystalline Cr:ZnSe sample. A thermal model is developed and predicts performance degradation at higher pump levels due to thermal quenching of the lifetime. This prediction is supported by the experimental results.

OCIS codes: (160.6990) Transition-metal-doped materials; (230.7380) Waveguides, channeled; (140.5680) Rare earth and transition metal solid-state lasers.

References

1. L. D. DeLoach, R. H. Page, G. D. Wilke, S. A. Payne, and W. F. Krupke, "Transition metal-doped zinc chalcogenides: spectroscopy and laser demonstration of a new class of gain media," IEEE J. Quantum Electron. **32**(6), 885–895 (1996).
2. R. H. Page, K. I. Schaffers, L. D. DeLoach, G. D. Wilke, F. D. Patel, J. B. Tassano, S. A. Payne, W. F. Krupke, K.-T. Chen, and A. Burger, "Cr^{2+}-doped zinc chalcogenides as efficient, widely tunable mid-infrared lasers," IEEE J. Quantum Electron. **33**(4), 609–619 (1997).
3. I. T. Sorokina, "Cr^{2+}-doped II-VI materials for lasers and nonlinear optics," Opt. Mater. **26**(4), 395–412 (2004).
4. P. A. Berry and K. L. Schepler, "High-power, widely-tunable $Cr^{(2+)}$:ZnSemaster oscillator power amplifier systems," Opt. Express **18**(14), 15062–15072 (2010).
5. T. J. Carrig, G. J. Wagner, W. J. Alford, and A. Zakel, "Chromium-doped chalcogenide lasers," SPIE Proceedings 5460 (2004).
6. E. Sorokin, I. T. Sorokina, M. S. Mirov, V. V. Fedorov, I. S. Moskalev, and S. B. Mirov, "Ultrabroad continuous-wave tuning of ceramic Cr:ZnSe and Cr:ZnS lasers," in Advanced Solid-State Photonics, San Diego, Ca. USA, AMC2 (2010).
7. G. J. Wagner, B. G. Tiemann, W. J. Alford, and T. J. Carrig, "Single-frequency Cr:ZnSe laser," in Advanced Solid-State Photonics, WB12 (2004).
8. M. N. Cizmeciyan, H. Cankaya, A. Kurt, and A. Sennaroglu, "Operation of femtosecond Kerr-lens mode-locked Cr:ZnSe lasers with different dispersion compensation methods," Appl. Phys. B **106**(4), 887–892 (2012).
9. K. L. Schepler, R. D. Peterson, P. A. Berry, and J. B. McKay, "Thermal Effects in Cr^{2+}:ZnSe thin disk lasers," IEEE J. Sel. Top. Quantum Electron. **11**(3), 713–720 (2005).
10. J. Nilsson and D. N. Payne, "Physics. High-power fiber lasers," Science **332**(6032), 921–922 (2011).
11. J. E. Williams, V. V. Fedorov, D. V. Martyshkin, I. S. Moskalev, R. P. Camata, and S. B. Mirov, "Mid-IR laser oscillation in Cr^{2+}:ZnSe planar waveguide," Opt. Express **18**(25), 25999–26006 (2010).
12. J. R. Sparks, R. He, N. Healy, M. Krishnamurthi, A. C. Peacock, P. J. A. Sazio, V. Gopalan, and J. V. Badding, "Zinc selenide optical fibers," Adv. Mater. **23**(14), 1647–1651 (2011).
13. J. R. Macdonald, R. R. Thomson, S. J. Beecher, N. D. Psaila, H. T. Bookey, and A. K. Kar, "Ultrafast laser inscription of near-infrared waveguides in polycrystalline ZnSe," Opt. Lett. **35**(23), 4036–4038 (2010).
14. J. R. Macdonald, S. J. Beecher, P. A. Berry, K. L. Schepler, and A. K. Kar, "Compact mid-infrared Cr:ZnSe channel waveguide laser," Appl. Phys. Lett. **102**(16), 161110 (2013).
15. J. R. Macdonald, S. J. Beecher, P. A. Berry, G. Brown, K. L. Schepler, and A. K. Kar, "Efficient mid-infrared Cr:ZnSe channel waveguide laser operating at 2486 nm," Opt. Lett. **38**(13), 2194–2196 (2013).
16. W. J. Tropf, "Temperature-dependent refractive index models of BaF_2, CaF_2, MgF_2, SrF_2, LiF, NaF, KCl, ZnS, and ZnSe," Opt. Eng. **34**(5), 1369–1373 (1995).
17. H. H. Li, "Refractive index of ZnS, ZnSe, and ZnTe and its wavelength and temperature derivatives," J. Phys. Chem. Ref. Data **13**(1), 103–150 (1984).

#192364 - $15.00 USD Received 17 Jun 2013; revised 1 Aug 2013; accepted 2 Aug 2013; published 8 Aug 2013

18. G. A. Slack, "Thermal conductivity of II-VI compounds and phonon scattering by Fe^{2+} impurities," Phys. Rev. **6**(10), 3791–3800 (1972).
19. G. C. Bhar, "Refractive index interpolation in phase-matching," Appl. Opt. **15**(2), 305–307 (1976).
20. A. Okhrimchuk, V. Mezentsev, A. Shestakov, and I. Bennion, "Low loss depressed cladding waveguide inscribed in YAG:Nd single crystal by femtosecond laser pulses," Opt. Express **20**(4), 3832–3843 (2012).

1. Introduction

Laser sources in the mid-IR region (2-5 μm) are of great interest for a number of commercial, military and scientific applications. Technologies such as remote chemical sensing, environmental monitoring, medical diagnostics, laser radar and molecular spectroscopy are some examples of the diverse applications driving research into compact, tunable and high power mid-IR sources.

Transition metal ions doped into II-VI semiconductors have many desirable laser medium qualities such as large absorption and emission bandwidths, large spin-allowed emission cross-sections, no excited state absorption (transitions to upper levels are spin forbidden) and room temperature operation [1–3]. Optical constants of several II-VI semiconductors of interest as transition metal hosts are given in Table 1. Cr^{2+}-doped ZnSe has been shown to be the most promising of these materials with demonstrations of high CW and pulsed output powers of 14 W and 18.5 W respectively [4,5], wide continuous tunability of 1973 – 3339 nm [6], narrow linewidth operation [7] and sub- 100 fs modelocked pulse durations [8]. Despite these achievements, the power scaling of these sources has long been impeded by thermal effects, in particular, the high thermo-optic coefficient (dn/dT) of Cr:ZnSe (see Table 1), 63 x 10^{-6} K^{-1}. Under high pump irradiances, thermal lensing occurs in the gain media causing cavity instability; this leads to decreasing laser output power (rollover) and even optical damage [9]. These thermal issues can be reduced but not eliminated by appropriate choices in pump wavelength, crystal geometry, heat removal techniques and master oscillator power amplifier (MOPA) configurations. These techniques have successfully pushed maximum CW output powers to above 10 Watts, but thermal effects have limited further power scaling [4].

A waveguide geometry can offer a significant reduction of difficulties caused by thermal lensing in the gain medium [10]. Planar waveguide lasing of Cr:ZnSe [11] has been demonstrated but with unreported laser output power. Channel waveguides provide the potential for lower thresholds, higher beam quality and maintenance of high gain over longer propagation distances by providing full two-dimensional transverse beam confinement. ZnSe optical fibers demonstrating low propagation losses have been manufactured [12], however transition metal doped ZnSe fiber lasing has not yet been reported. Ultrafast laser inscription has been reported as a viable method for waveguide fabrication in ZnSe substrates [13], and the technology was used in the fabrication of the first Cr:ZnSe channel waveguide laser [14]. These initial structures were used to demonstrate an output power of 18.5 mW for a pump power of ~1200 mW utilizing a double depressed cladding structure [14]. A significant improvement in waveguide fabrication resulted in a maximum power output of 285 mW and slope efficiencies as high as 45% [15]. In this paper we report a six-fold increase in laser output power and present modeling of power scaling with attention to issues expected to ultimately limit waveguide laser power in TM-doped II-VI host materials.

#192364 - $15.00 USD Received 17 Jun 2013; revised 1 Aug 2013; accepted 2 Aug 2013; published 8 Aug 2013

Table 1. Optical constants of II-VI materials[a]

Material	Refractive index *n @ 2.5 μm*	*dn/dT @ 2.5 μm* *(10^{-6}/K)*	Thermal conductivity *mW/(cm*K)*	Trans-mission range *(μm)*	Bandgap[b] *(eV)*	Density[b] *(g/cm^3)*	Cations[c] *(10^{22}cm^{-3})*
ZnS	2.260 [16]	43 [16]	270 [18]	0.4-12	3.54	4.09	2.52
ZnSe	2.441 [16]	63 [16]	190 [18]	0.6-15	2.82	5.27	2.19
ZnTe	2.711 [17]		180 [18]	0.6-20	2.24	5.63	1.75
CdSe	2.548(o) [19] 2.480 (e) [19]			0.7-20	1.74	5.82	1.82

[a]all values quoted for room temperature and zinc blende structure except wurtzite structure CdSe
[b]from multiple commercial vendors.
[c]knowing the number of cations is useful for converting between dopant concentrations in absolute density and atomic substitution fraction.

2. ZnSe waveguide fabrication

Waveguides were inscribed using 750 fs pulses at 100 kHz repetition rate from a Yb:fiber chirped pulse amplifier system (IMRA μJewel D400) with a range of pulse energies of 1–2.55 μJ investigated. These pulses were focused into an 8.5 x 6.5 x 2.1 mm polycrystalline Cr:ZnSe sample, doped to 7 x 10^{18} cm^{-3}(320 ppm) with Cr ions, using a 0.6 NA objective. The sample was translated through the beam at velocities ranging from 0.5 – 27 mm/s.

The structure design consisted of a depressed annular cladding region surrounding an undamaged core similar to that first demonstrated in Nd:YAG by Okhrimchuk *et al.* [20]. Multiple elements of reduced refractive index were inscribed, forming a circular cross-section as shown in Fig. 1 (left). In early attempts to inscribe ZnSe, we observed non-uniform structures consisting of multiple self-focusing and de-focusing regions. This effect, due to the high $\chi^{(3)}$ nonlinearity of ZnSe, was mitigated by using pulses which were deliberately stretched temporally to 750 fs. This longer pulse length increased the pulse energy allowed before reaching the self-focusing peak-power threshold. Due to the high threshold for modification, each element was formed by multiple passes of the substrate through the laser focus, producing a result in Cr:ZnSe as seen in Fig. 1 (right) for a 120 μm diameter design.

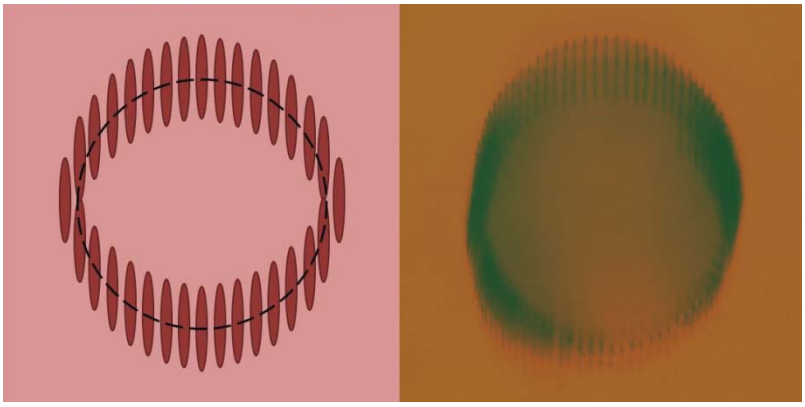

Fig. 1. Circular cross-section, depressed-index cladding waveguide design (left) and 120 μm diameter sample (right), composed of individual modified regions (dark) created via ultrashort pulse laser inscription in unmodified material (light).

In addition to the parameters detailed above, the diameter, number of elements in each waveguide and the number of translations of the sample through the focus to create each element were investigated. Structures with diameters of 40, 60, 80, 120, 160 and 200 μm were fabricated with a range of component elements numbering from 40 to 120 and number of sample translations per element between 1 and 51. After inscription, the sample end facets

#192364 - $15.00 USD Received 17 Jun 2013; revised 1 Aug 2013; accepted 2 Aug 2013; published 8 Aug 2013

were ground back and polished to remove any surface damage and waveguide tapering due to the inscription beam transitioning on and off the sample during fabrication leaving waveguides of 6.0 mm length.

3. Power scaling of Cr:ZnSe waveguide lasers

We previously reported demonstration of an 18.5 mW laser based on a rectangular Cr:ZnSe channel waveguide structure with an inner (low index change) and outer cladding (high index change) for beam confinement [14]. A depressed annular cladding region surrounding an undamaged core as described in Section 2 provided improved laser performance. Maximum power output of 285 mW was achieved and slope efficiencies as high as 45% were demonstrated. Output power was limited only by available pump power of 1.1 W and showed no signs of thermal rollover. Losses in the waveguides were calculated to be 0.7 dB/cm at the lasing wavelength of 2485 nm [15].

To scale to the higher powers reported in this paper, a sample containing a range of inscribed waveguide structures was inserted into a cavity depicted in Fig. 2. This cavity consisted of a planar dichroic input coupler (transmission > 98% at 1908 nm, reflectivity > 99% at 2450 nm) and a planar output coupler, both mounted with independent tip/tilt control and the ability to translate along the beam propagation axis. The Cr:ZnSe crystal was anti-reflection (AR) coated on both sides for 1900-3000 nm wavelengths and mounted to a water-cooled aluminum block kept at 15 °C and capable of pitch/yaw adjustment and translation transverse to the beam propagation axis. This system enabled the sample to be positioned for optimal coupling into a particular waveguide and then for the aligned cavity mirrors to be brought in very close to the crystal surface. Pump power was coupled into the cavity using various lenses designed to match the mode field diameter of the waveguides and AR coated for the pump wavelength. Output from the cavity was collimated using a calcium fluoride lens AR coated from 1900 to 3000 nm. A second dichroic mirror outside the cavity was used to dump unabsorbed pump power.

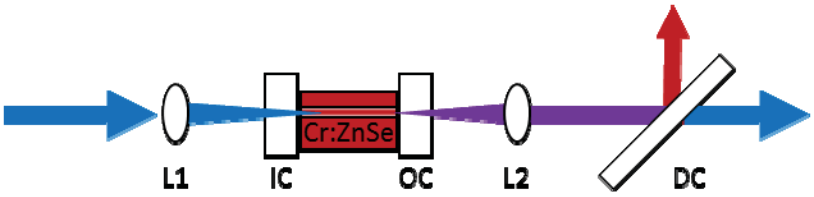

Fig. 2. Waveguide laser cavity configuration consisting of pump lens (L1), input and output couplers (IC/OC) surrounding the Cr:ZnSe waveguide crystal, output collimating lens (L2) and a dichroic mirror to separate residual pump and laser output (DC).

The sample was optically pumped with an IPG thulium fiber laser with a maximum available power of 38 W at 1908 nm. Waveguide lasing was investigated for output couplers with reflectivities (R) of 50%, 70%, 80% and 90%. Pure continuous-wave lasing was observed for a number of waveguide structures, but the highest power output was obtained from a waveguide with an 80 μm design diameter consisting of 60 elements each made up of 25 sample translations per element. This waveguide is assumed to have losses comparable with those of similar waveguides previously reported by Macdonald et al. [15]. The input-output characteristics of the laser for different output couplers can be seen in Fig. 3. The input powers and thresholds shown are in terms of power incident on the front face of the crystal. A portion of the pump power is not absorbed, thus the slope efficiency values are a low estimate. A maximum output power of 1.7 W was achieved with 9.3 W of incident pump power.

#192364 - $15.00 USD Received 17 Jun 2013; revised 1 Aug 2013; accepted 2 Aug 2013; published 8 Aug 2013

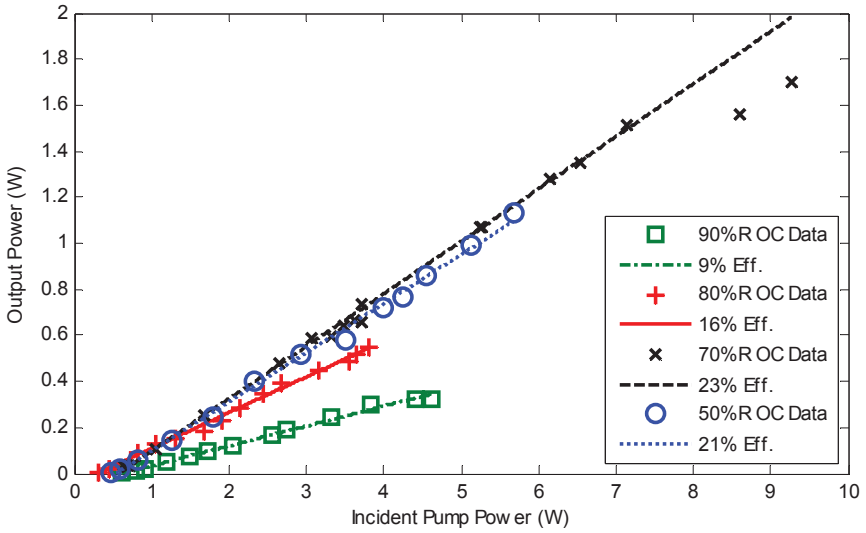

Fig. 3. Laser performance for varying output coupler reflectivities.

The output spectra of the laser under 80%, 70% and 50% reflective output coupling were measured with an Acton Research Corporation 750 mm monochromator and an extended range InGaAs detector. The spectra are shown in Fig. 4 below, along with the spectral reflectivity performance of the corresponding output couplers and the input coupler. All three laser configurations exhibit relatively narrow (~10 nm) linewidths near the peak gain of Cr:ZnSe (2450 nm) but shifted slightly due to the effect of the input and output couplers.

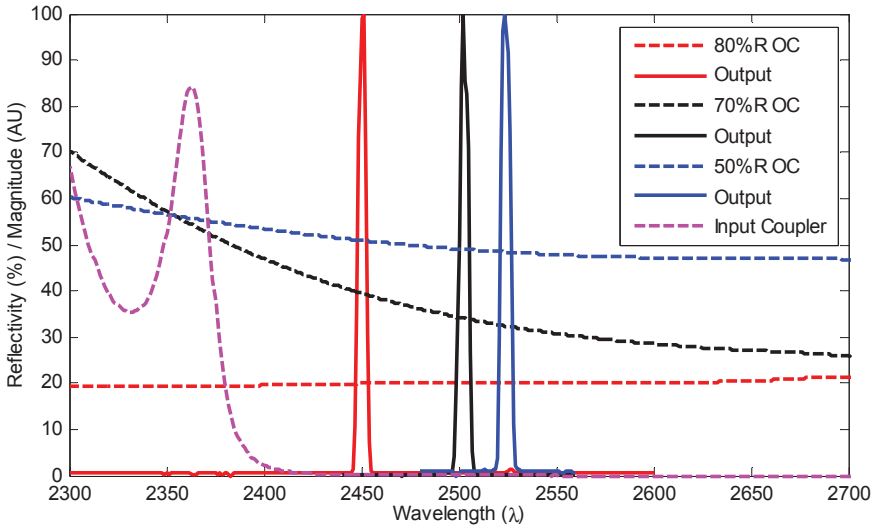

Fig. 4. Spectral response of laser system overlaid with spectral reflectivity response of cavity mirrors.

4. Modeling of Cr:ZnSe waveguide laser performance

While waveguide confinement mitigates thermal lensing issues in Cr:ZnSe, the tight confinement exacerbates the issue of non-radiative quenching. A certain fraction of pump power is converted into heat even in the case of lasing [9] and as the temperature of the ZnSe

#192364 - $15.00 USD Received 17 Jun 2013; revised 1 Aug 2013; accepted 2 Aug 2013; published 8 Aug 2013

host material rises above room temperature the non-radiative relaxation rate rises rapidly [2]. Tight confinement leads to high temperatures even at moderate pumping powers.

The temperature rise in the waveguide structure described in Section 2 was calculated using COMSOL®. A waveguide structure similar to that used experimentally was modeled with an 80 μm diameter located 200 μm from a single cooled surface. Laser pumping was calculated for a Gaussian beam with 40 μm $1/e^2$ radius points and with 320 ppm Cr doping. Beer's law heat deposition was calculated using an absorption cross section of 1 x 10^{-18} cm^2 for 1.9 μm pumping. The model calculated a 19 K temperature increase per watt of incident power. This is the maximum temperature increase at the front of the waveguide as shown in Fig. 5. The modeled ZnSe crystal length was cut off at 500 μm to better observe the worst case situation at the front of the waveguide.

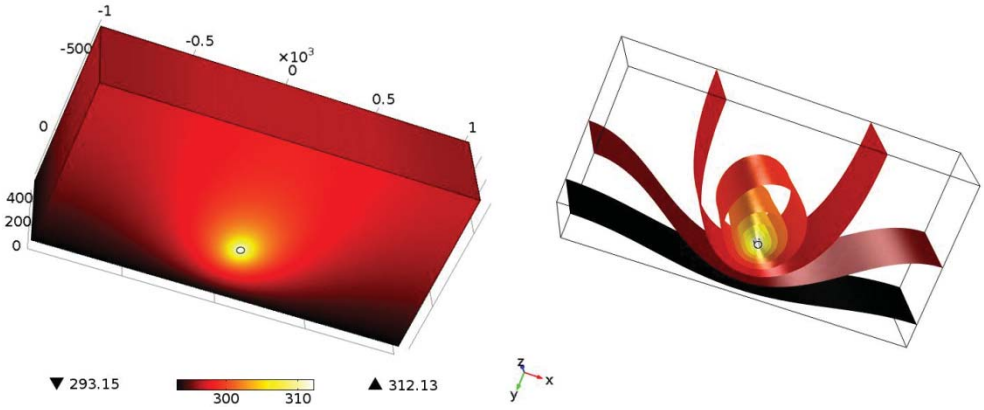

Fig. 5. Plots of calculated temperature of a Cr:ZnSe slab pumped by a Gaussian beam with 40 μm $1/e^2$ radii propagating along a 40 μm radius waveguide structure. The bottom dark surface was fixed at room temperature to simulate mounting on a heat sink. The left plot is a surface plot of temperature; the right plot is an isosurface plot of the region near the waveguide region. The dimensions and location of the waveguide region were chosen to match those of the actual waveguide sample used to demonstrate lasing except for the waveguide propagation length (0.5 mm rather than the actual 6 mm length).

Lasing operation is expected to reduce the heat load but at a certain point of pumping the situation will become unstable. A small increase in temperature will lead to an increased rate of non-radiative relaxation which in turn leads to decreased lasing and greater temperature rise. This feedback can continue until lasing stops completely. An approximate calculation of the above-threshold pump power at which lasing ceases can be done by recalling that

$$P_{out} = S\left(P_{in} - P_{th}\right) \tag{1}$$

where P_{out} is the laser output power, P_{in} is the laser pump power, P_{th} is the laser threshold power and S is the slope efficiency. For a four-level laser,

$$P_{th} = \kappa\left(I_{sat}\right) \tag{2}$$

where I_{sat} is the saturation intensity dependent only on the physics of Cr^{2+} ions and κ is a proportionality constant that depends upon details of a specific laser resonator setup. Saturation intensity in our case depends upon temperature since emission lifetime depends on temperature, i.e.,

$$I_{sat}\left(T\right) = \frac{h\upsilon_e}{\sigma_e \tau\left(T\right)} \tag{3}$$

#192364 - $15.00 USD Received 17 Jun 2013; revised 1 Aug 2013; accepted 2 Aug 2013; published 8 Aug 2013

where h is Planck's constant, ν_e is the frequency of the emitted photon, σ_e is the emission cross section and $\tau(T)$ is the emission lifetime. Note that for Cr:ZnSe as we increase pump power we expect τ to rapidly decrease as the temperature goes above 300 K. That means that I_{sat} and P_{th} increase. Eventually output power will no longer increase with increasing pump power at a critical pump power so that

$$0 = \frac{dP_{out}}{dP_{in}} = S\left(1 - \frac{dP_{th}}{dP_{in}}\right) \tag{4}$$

where the right side of Eq. (4) comes from differentiating Eq. (1) with respect to input power. Solving for dP_{th}/dP_{in} and using

$$\frac{dP_{th}}{dP_{in}} = \kappa \frac{dI_{sat}}{dT}\frac{dT}{dP_{in}} \tag{5}$$

we have

$$\frac{\kappa h \upsilon_e}{\sigma_e}\frac{d(1/\tau)}{dT}\frac{dT}{dP_{in}} = 1 \tag{6}$$

Experimental measurements of lifetime, τ, were fit to a 4th order polynomial for convenience, no phenomenological significance intended, in order to calculate the temperature derivative of 1/τ. The dT/dP_{in} factor is equal to the model calculation of H = 19 K/W shown in Fig. 5. Below lasing threshold $dT/dP_{in} = H$. Above threshold, there is less heating since there is less chance for non-radiative relaxation; so $dT/dP_{in} = (1\text{-}S)H$. Figure 6 shows a plot of the left side of Eq. (6) for the Cr:ZnSe waveguide laser reported in [15].

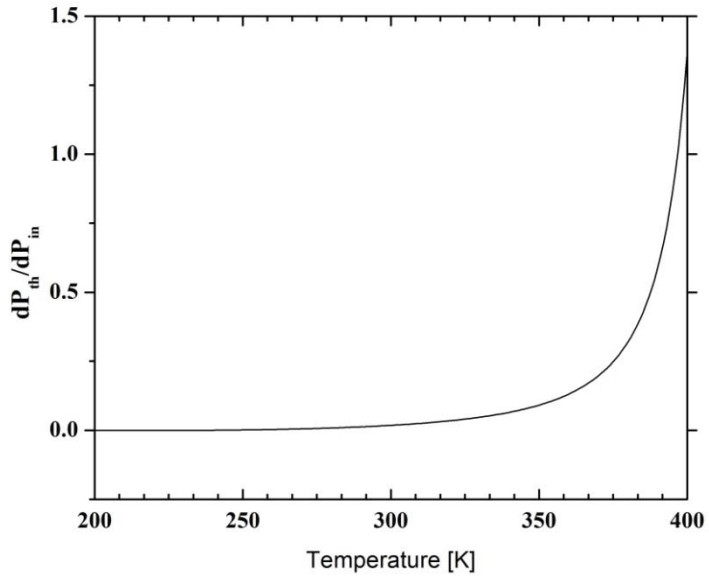

Fig. 6. Calculation of change in lasing threshold power with respect to change in incident pump power as a function of temperature for the waveguide laser described in [15].

#192364 - $15.00 USD Received 17 Jun 2013; revised 1 Aug 2013; accepted 2 Aug 2013; published 8 Aug 2013

We have a solution of Eq. (6) at a critical temperature of ~395K. The critical change in temperature $\Delta T_{crit} = T_{crit} - T_o$ where T_o is the heat sink temperature is given in terms of input power by

$$\Delta T_{crit} = \frac{dT}{dP_{in}} P_{th} + (1 - S) \frac{dT}{dP_{in}} (P_{crit} - P_{th}) \tag{7}$$

Solving this equation for critical incident pump power, P_{crit} gives

$$P_{crit} = \frac{\Delta T_{crit} - S P_{th} \dfrac{dT}{dP_{in}}}{(1 - S) \dfrac{dT}{dP_{in}}} \tag{8}$$

For an 80 μm diameter waveguide using a 90% R output coupler, S = 0.09, P_{th} = 0.62 W, ΔT_{crit} = 106 K and dT/dP_{in} = 19 K/W, we calculate a critical incident pump power of approximately 6.1 W. Note that this is the critical power for the front region of the waveguide; regions further downstream will reach critical temperature at slightly higher powers. However, loss of lasing emission from the front region will make extraction efficiency poorer in downstream regions leading to more heating in these regions and abrupt quenching of laser emission. As can be seen in Fig. 3 above, the power in this particular waveguide does start to roll over at around 4 W of incident pump power. For the 70% R output coupler results, output drops at 7 W while the model gives a prediction of 6.8 W. Thus the model and experimental results are in good agreement.

Note that we also expect a hysteresis effect if we turn down power after quenching lasing; lasing will only be restored at a temperature (or power) lower than the critical level because no lasing produces more heating. Thus incident power must be reduced to the point where temperature is below the critical temperature with no lasing present. This is equivalent to setting S = 0 in Eq. (8) and gives a incident pump power for restoration of lasing of 5.3 W for the 90% R output coupler and 5.8 W for the 70% R output coupler.

Further scaling of waveguide output power will require mitigation of thermal quenching of lasing. Several approaches can be considered. Cooling the waveguide would increase the temperature change needed to reach the point of thermal quenching but by only a factor of 3.2 with liquid nitrogen cryo-cooling. Such an approach is not desirable considering the added complexity. Another approach is to increase the waveguide diameter. Spreading the heat over a larger area will reduce dT/dP_{in} by a factor proportional to the diameter squared. However, increasing the waveguide area may also reduce the beam quality. Temperature increase can also be reduced by reducing the Cr^{2+} dopant concentration in the ZnSe host material. However, this will reduce the gain per unit length and lasing requires that gain per unit length be larger than loss per unit length. Thus efforts to reduce waveguide loss will be highly beneficial. Reduced waveguide loss will not only allow more efficient laser operation, it will also enable further Cr laser power scaling.

Finally, the buried waveguide structure could be moved closer to the heatsink surface. Locating the waveguide structure center 100 μm instead of 200 μm away from the heatsink reduced dT/dP_{in} from 19.0 to 12.7 and increased critical incident power for the 70% R output coupler case from 6.8 W to 10.7 W in the model. A judicious combination of these power scaling approaches should easily allow for order of magnitude scaling of waveguide output power.

#192364 - $15.00 USD Received 17 Jun 2013; revised 1 Aug 2013; accepted 2 Aug 2013; published 8 Aug 2013

5. Summary

Ultrafast laser inscription techniques were developed and refined to produce structures in Cr:ZnSe laser materials. These waveguides were shown to support power scaling of laser output up to 1.7 W with performance limited by thermal quenching of lifetime. A thermal model was developed which successfully predicts this performance degradation at higher pump levels. Further power scaling should be possible through appropriate modifications of waveguide structure and Cr^{2+} doping. Future work in this area will focus on improving the losses and reducing temperature rise in the structures.

Acknowledgments

This work was supported by the U.S. Air Force Office of Scientific Research, the U.S. Air Force Research Laboratory Sensors Directorate, contract number FA8650-12-D-1377, the European Office of Aerospace Research and Development (EOARD) grant number FA8655-11-1-3001 and the Engineering and Physical Sciences Research Council (EPSRC) grant number EP/G030227/1. J.R.M. and S.J.B. thank Graeme Brown for his assistance in the waveguide inscription process.

#192364 - $15.00 USD Received 17 Jun 2013; revised 1 Aug 2013; accepted 2 Aug 2013; published 8 Aug 2013